DOI: 10.1534/genetics.110.117341

A Ubiquitin E2 Variant Protein Acts in Axon Termination and Synaptogenesis in *Caenorhabditis elegans*

Gloriana Trujillo,*,[1] Katsunori Nakata,[1,2,†] Dong Yan,*,[‡] Ichi N. Maruyama[†] and Yishi Jin*,[‡,3]

**Neurobiology Section, Division of Biological Sciences, University of California, San Diego, CA 92093 †Information Processing Biology Unit, Okinawa Institute of Science and Technology, Onna-Son, Okinawa 904-0412, Japan and ‡Howard Hughes Medical Institute, La Jolla, CA 92093*

Manuscript received April 8, 2010
Accepted for publication June 19, 2010

ABSTRACT

In the developing nervous system, cohorts of events regulate the precise patterning of axons and formation of synapses between presynaptic neurons and their targets. The conserved PHR proteins play important roles in many aspects of axon and synapse development from *C. elegans* to mammals. The PHR proteins act as E3 ubiquitin ligases for the dual-leucine-zipper-bearing MAP kinase kinase kinase (DLK MAPKKK) to regulate the signal transduction cascade. In *C. elegans,* loss-of-function of the PHR protein RPM-1 (Regulator of Presynaptic Morphology-1) results in fewer synapses, disorganized presynaptic architecture, and axon overextension. Inactivation of the DLK-1 pathway suppresses these defects. By characterizing additional genetic suppressors of *rpm-1*, we present here a new member of the DLK-1 pathway, UEV-3, an E2 ubiquitin-conjugating enzyme variant. We show that *uev-3* acts cell autonomously in neurons, despite its ubiquitous expression. Our genetic epistasis analysis supports a conclusion that *uev-3* acts downstream of the MAPKK *mkk-4* and upstream of the MAPKAPK *mak-2*. UEV-3 can interact with the p38 MAPK PMK-3. We postulate that UEV-3 may provide additional specificity in the DLK-1 pathway by contributing to activation of PMK-3 or limiting the substrates accessible to PMK-3.

CHEMICAL synapses are specialized cellular junctions that enable neurons to communicate with their targets. An electrical impulse causes calcium channel opening and consequently stimulates synaptic vesicles in the presynaptic terminals to fuse at the plasma membrane. Neurotransmitter activates receptors on the postsynaptic membrane and triggers signal transduction in the target cell. For this communication to occur efficiently, the organization of the proteins within these juxtaposed pre- and postsynaptic terminals must be tightly regulated (Jin and Garner 2008). Previous studies in *Caenorhabditis elegans* have identified RPM-1, a member of the conserved PHR (Pam/Highwire/RPM-1) family of proteins, as an important regulator for the synapse (Schaefer *et al.* 2000; Zhen *et al.* 2000). Recent functional studies of other PHR proteins have shown that they are also required for a number of steps during nervous system development including axon guidance, growth, and termination (Wan *et al.* 2000; D'souza; *et al.* 2005; Bloom *et al.* 2007; Grill *et al.* 2007; Lewcock *et al.* 2007; Li *et al.* 2008).

The signaling cascades regulated by the PHR proteins have been identified using genetic modifier screens (Diantonio *et al.* 2001; Liao *et al.* 2004; Nakata *et al.* 2005; Collins *et al.* 2006) and biochemical approaches (Grill *et al.* 2007; Wu *et al.* 2007). These studies reveal that a major function of PHR proteins is to act as ubiquitin E3 ligases (Jin and Garner 2008). In *C. elegans*, RPM-1 (Regulator of Presynaptic Morphology-1) regulates the abundance of its substrate, the dual-leucine-zipper-bearing MAP kinase kinase kinase (DLK MAPKKK), and controls the activity of the MAP kinase cascade composed of three additional kinases, MAPKK MKK-4, p38 MAPK PMK-3, and MAPKAPK MAK-2 (Nakata *et al.* 2005; Yan *et al.* 2009). This signaling cascade further regulates the activity of the CCAAT/enhancer binding protein (C/EBP), CEBP-1, via a mechanism involving 3′-UTR-mediated mRNA decay.

Signal transduction involving MAP kinases can be fine tuned using multiple mechanisms to ensure optimal signaling outputs (Raman *et al.* 2007). For example, scaffold proteins for MAP kinases can provide spatial regulation of kinase activation in response to different stimuli (Remy and Michnick 2004; Whitmarsh 2006). Small protein tags such as ubiquitin have also been shown to control the activation of kinases. Specifically, in the IKK pathway ubiquitination via Lys63 chain

Supporting information is available online at http://www.genetics.org/cgi/content/full/genetics.110.117341/DC1.

[1] These authors contributed equally to this work

[2] *Present address:* Research Institute of Pharmaceutical Sciences, Musashino University, Tokyo 202-8585, Japan.

[3] *Corresponding author:* 9500 Gilman Dr., MC 0368, University of California, San Diego, CA 92093-0368. E-mail: yijin@ucsd.edu

formation catalyzed by the Ubc13/Uev1a E2 complex and TRAF6 E3 ligase is required for TAK1 kinase activation (Skaug *et al.* 2009).

To further the understanding of the DLK-1 pathway in the development of the nervous system, we characterized a new complementation group of *rpm-1(lf)* suppressors. These mutations affect the gene *uev-3*, a ubiquitin E2 conjugating (UBC) enzyme variant (UEV). UEV proteins belong to the UBC family, but lack the catalytic active cysteine necessary for conjugating ubiquitin (Sancho *et al.* 1998). The best characterized UEV proteins are yeast Mms2 and mammalian Uev1A, both of which act as the obligatory partner for the active E2 Ubc13 and function in DNA repair and IKB pathways, respectively (Deng *et al.* 2000; Hurley *et al.* 2006). In addition, UEV proteins, such as Tsg101, can also regulate endosomal trafficking (Babst *et al.* 2000). We find that similar to other members of the DLK-1 pathway, *uev-3* functions cell autonomously in neurons. *uev-3* genetically acts downstream of *mkk-4* and upstream of *mak-2*. UEV-3 can bind PMK-3 in heterologous protein interaction assays. We hypothesize that UEV-3 may add specificity to the DLK-1 pathway by binding to PMK-3 for its activation or for selecting specific downstream targets.

MATERIALS AND METHODS

***C. elegans* genetics:** *C. elegans* strains were maintained as described (Brenner 1974). The suppressors were isolated from *rpm-1(ju44); syd-2(ju37); juIs1* or *rpm-1(ju44); syd-1(ju82); juIs1* animals mutagenized with 50 mm EMS (Nakata *et al.* 2005). Suppressor mutations were outcrossed multiple times against wild-type (N2) or *juIs1[Punc-25 SNB-1::GFP]* strains. Specificity of suppression of *rpm-1(lf)* was tested by crossing *sup; rpm-1; syd-2; juIs1* to *rpm-1; juIs1* males. Double mutants were constructed following standard procedures, and the genotypes were confirmed by allele-specific nucleotide alterations determined by DNA sequencing or restriction enzyme digest.

Cloning of *uev-3*: We mapped the suppression activity of *uev-3(ju587)* in the *rpm-1; syd-2* double mutant strain to chromosome I near +4 using the single-nucleotide polymorphism mapping strategy (Davis *et al.* 2005; Nakata *et al.* 2005). For fine mapping of *uev-3 (ju587)*, we constructed *dpy-5 uev-3 (ju587) unc-75; rpm-1; juIs1* strain. Following crossing to the Hawaiian strain CB4856, recombinant animals of phenotypic Dpy non-Unc or Unc non-Dpy that were mutant for *rpm-1* were selected, and the presence of *uev-3 (ju587)* in each recombinant was determined by observing *juIs1* marker expression. *uev-3 (ju587)* was mapped between *snp_F14B4[1]* and *snp_M04C9[1]*, within a 90-kb interval including about 19 predicted genes. We performed RNAi against the predicted genes using a sensitized strain *eri-1(mg366); rpm-1(ju23); syd-2(ju37)*, and found that *uev-3* RNAi caused suppression of *rpm-1; syd-2* phenotypes. *ju593*, *ju638*, and *ju639* were determined to be alleles of *uev-3* on the basis of linkage to chromosome I and noncomplementation test. DNA sequence analyses of these suppressor mutations were carried out following standard procedures, and the nucleotide alterations were confirmed in independent PCR reactions.

Molecular biology and expression constructs: We determined the gene structure and the full-length transcripts of *uev-3* by RT–PCR and 5′-RACE analyses. Total RNAs were prepared using TRIzol reagents (Invitrogen, Carlsbad, CA) according to the manufacturer's instructions, and cDNAs were generated using Superscript II reverse transcriptase (Invitrogen, Carlsbad, CA). The 5′-RACE kit (Roche Applied Science, Indianapolis, IN) was used with the following pair of primers to amplify the 5′ region of *uev-3:* SP1 and YJ3861 ccattga cacgttgagattc and SP2 and YJ3846 acgtttagacactcctccc. DNA sequence analysis of eight cloned 5′-RACE products revealed a SL2 splice leader in all, indicating that *uev-3* is transcribed as the downstream gene in the operon with *rab-5*. We obtained full-length *uev-3* cDNA by RT–PCR using YJ3852 gggga caagtttgtacaaaaaagcaggctccaaaatgtccgatcaacctgg and YJ3853 ggggaccactttgtacaagaaagctgggttatgaaattccaatgacatc. The DNA sequences of the cDNA clone (pCZ729) verified and corrected the predicted *uev-3* exon and intron boundaries. The *uev-3* expression constructs in *C. elegans* were generated following standard procedures or using Gateway Cloning Technology (Invitrogen, Carlsbad, CA), and the details of the clones are in supporting information, Table S2. For yeast two-hybrid studies, full-length cDNA or fragments of cDNA for *dlk-1*, *mkk-4, pmk-3, mak-2,* or *uev-3* were cloned either to pBTM116 vector to be expressed as GAL4 activation domain fusion protein or into pACT2 vector to be expressed as LexA DNA binding domain fusion protein, as described in Table S2. To generate pcDNA3-HA-uev-3 (pOF174), *uev-3* cDNA was cloned into pcDNA3-HA-Gateway (pOF173) vector by Gateway system. To generate pFLAG-CMV-2-pmk-3 (pOF171), *pmk-3* cDNA was cloned into pFLAG-CMV-2-Gateway (pOF169) vector by Gateway system. pFLAG-CMV-2-pmk-3 (AQF) (pOF175) was generated by PCR-based mutagenesis to change the TQY dual phosphorylation site to AQF.

Neuronal morphology and synapse analyses: We observed GFP or SNB-1::GFP using *muIs32[Pmec-7-GFP] or juIs1[Punc-25-SNB-1::GFP]* in 1-day-old adult animals either live or anesthetized in 1% 1-phenoxy-2-propanol (TCI America, Portland, OR) in M9 buffer. Images were captured either on a Zeiss Axioplan 2 microscope with Chroma HQ filters or a Zeiss LSM510 confocal microscope.

Germline transformation and transgenic analyses: Transgenic animals were usually generated by injecting DNA at a dilution series (1–50 ng/μl) following standard procedures (Mello *et al.* 1991), using either pRF4 *rol-6(dm)* or *Pttx-3-RFP* as coinjection markers. For each construct, 2 to 13 independent transgenic lines were analyzed.

Yeast two hybrid: Yeast two-hybrid assays were performed using pACT2 and pBTM116 vector backbones (Clontech, Mountain View, CA). The yeast strain L40 [*MATa his3D200 trp1-901 leu2-3, 112 ade2 LYS2::(lex-Aop)4-HIS3 URA3::(lex-Aop)8-lacZ GAL4 gal80*] was used. The yeast transformation was performed by the lithium acetate method and selected on Trp-, Leu-, and His-selection plates. Pairs of plasmids were cotransformed into yeast strain L40, and selected on Leu–Trp plates. For interaction assay, single clones were picked from each transformation and cultured to $OD_{600} = 1$. Yeast cells were pelleted by centrifugation, washed three times and resuspended, and plated in a dilution series of 10 to 10000 times by pipeting 5 μl per spot onto Histidine selection plates containing 3mm 3-AT. β-Galactosidase assays were performed following the Clontech Yeast Protocols Handbook (Fields and Sternglanz 1994).

***cebp-1* mRNA analysis by qRT–PCR:** RNA isolation and cDNA preparation were performed as above. Power SYBR Green PCR Master Mix kits (Applied Biosystems, Foster City, CA) were used for the PCR reactions and the ABI Prism 7000 Sequence Detection system was used for real-time PCR. cDNAs were amplified using following primers: *cebp-1* pair (gcacga caagatgaagagg and gcatgcgttgctctttca) amplifies 183 bp; *ama-1*

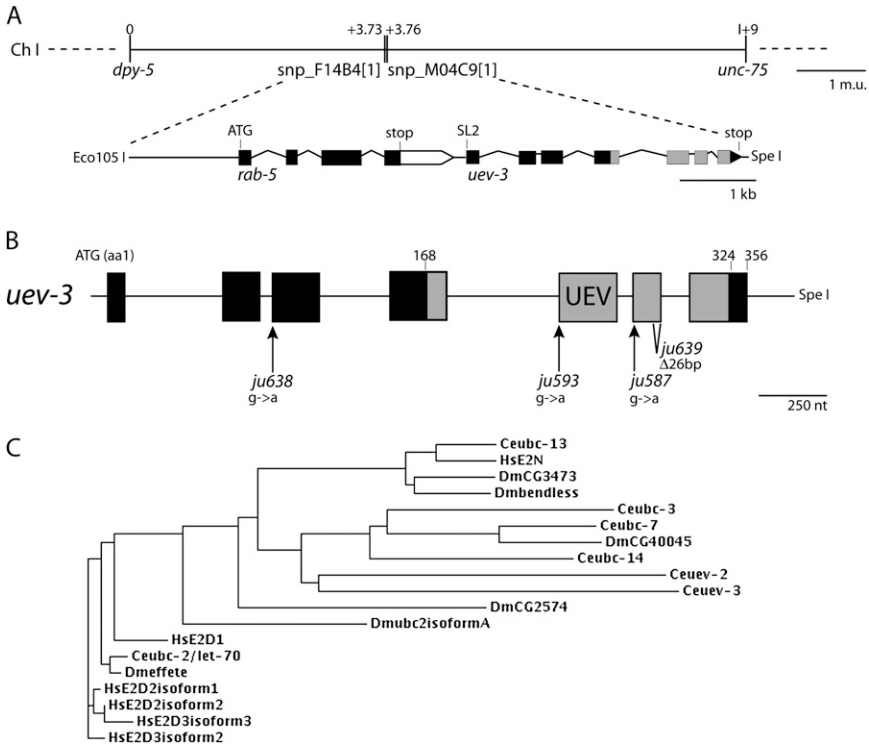

FIGURE 1.—*uev-3* is a ubiquitin E2 variant. (A) *uev-3* locus on chromosome I. The *Eco*1051–*Spe*I genomic fragment from cosmid F26H9 fully rescues the suppression of *rpm-1(lf)* by *uev-3* mutations. Solid box, coding sequences; open box, 3′ UTR; and lines, promoter or intronic sequences. (B) Illustration of *uev-3* gene structure and positions of the mutations. Solid boxes, exons; and shading, UEV domain. (C) Dendrogram of UEV-3 with close homologs (ClustalW) *Ce, C. elegans; Dm, Drosophila melanogaster,* and *Hs, Homo sapiens.*

pair (actcagatgacactcaacac and gaatacagtcaacgacggag) amplifies 128 bp.

Protein interaction studies in 293T mammalian cells: Human embryonic kidney 293T cells were maintained in Dulbecco's modified Eagle's medium (DMEM) supplemented with 10% fetal calf serum. Cells were transfected with a total of 5 μg of DNA containing various expression vectors. After 24 hr, cells were collected and washed once with phosphate-buffered saline (PBS) and lysed in 0.4 ml of 0.1% NP-40 lysis buffer (20 mM HEPES, pH 7.4, 150 mM NaCl, 1.5 mM $MgCl_2$, 2 mM EGTA, 2 mM dithiothreitol, protease inhibitor, Roche Applied Science, Indianapolis, IN, and phosphatase inhibitor,Nacalai, San Diego, CA). Cellular debris was removed by centrifugation at 10,000 × *g* for 5 min. FLAG epitope-tagged proteins were immunoprecipitated with anti-FLAG monoclonal antibody M2 (Sigma, St. Louis, MO). For immunoblotting, aliquots of immunoprecipitates and whole-cell lysates were resolved on SDS–polyacrylamide gel electrophoresis (SDS–PAGE), and transferred to Amersham Hybond-P membranes (GE Healthcare, Piscataway, NJ). The membranes were immunoblotted with anti-HA rabbit polyclonal antibody Y-11 (Santa Cruz Biotechnology Inc., Santa Cruz, CA). The bound antibody was visualized with horseradish peroxidase-conjugated antibody to rabbit IgG using the Amersham ECL Advance Western blotting detection kit (GE Healthcare, Piscataway, NJ).

RESULTS

UEV-3 is a Ubc/E2 variant protein: Previous analyses of the suppressors of *rpm-1* loss-of-function (lf) mutants revealed five loci, defining *dlk-1*, *mkk-4*, *pmk-3*, *mak-2*, and *cebp-1* (NAKATA *et al.* 2005; YAN *et al.* 2009). We devised a noncomplementation test scheme and identified four alleles belonging to a new complementation group: *ju593*, *ju587*, *ju638*, and *ju639*. We mapped this suppressor locus to an interval of ~90 kb on the right arm of chromosome I (Figure 1A). We used a combination of RNAi and transgenic expression of cosmid DNAs from the region to locate the gene affected. We found that the 6-kb *Eco*105I–*Spe*I fragment of the cosmid F26H9 contained the rescuing activity for the suppression of *rpm-1(ju44)* by *ju587*. The genomic DNA fragment contains two predicted genes: *rab-5* and *uev-3*. By RT–PCR and 5′-RACE analyses, we determined that *uev-3* transcripts contained an SL2 splice leader, confirming that *rab-5* and *uev-3* form an operon, with *uev-3* as the downstream gene (MATERIALS AND METHODS). DNA sequence analysis from *ju587*, *ju593*, and *ju638* identified single nucleotide alteration at various splice acceptor sites, while *ju639* is a 26-bp deletion from amino acid 277 in the sixth exon (Figure 1B and Table S1). Moreover, we performed RNAi of *uev-3* in a sensitized genetic background and observed partial suppression of *rpm-1(lf)* (Table S1). These analyses are consistent with the suppressor mutations causing loss-of-function in *uev-3*.

uev-3 is one of the three UEV proteins in *C. elegans* (JONES *et al.* 2002; KIPREOS 2005). It is composed of 356 amino acids, with the UEV domain from residues 168 to 324 (Figure 1B). UEV proteins are similar to UBC E2 enzymes but lack the critical cysteine residue that is required for a transient interaction between E2 and ubiquitin (SANCHO *et al.* 1998; PICKART and EDDINS 2004) (Figure S1). Alignment of the UEV domain of UEV-3 with other UBC and UEV proteins reveals motifs with high similarity; for example, the HxN tripeptide

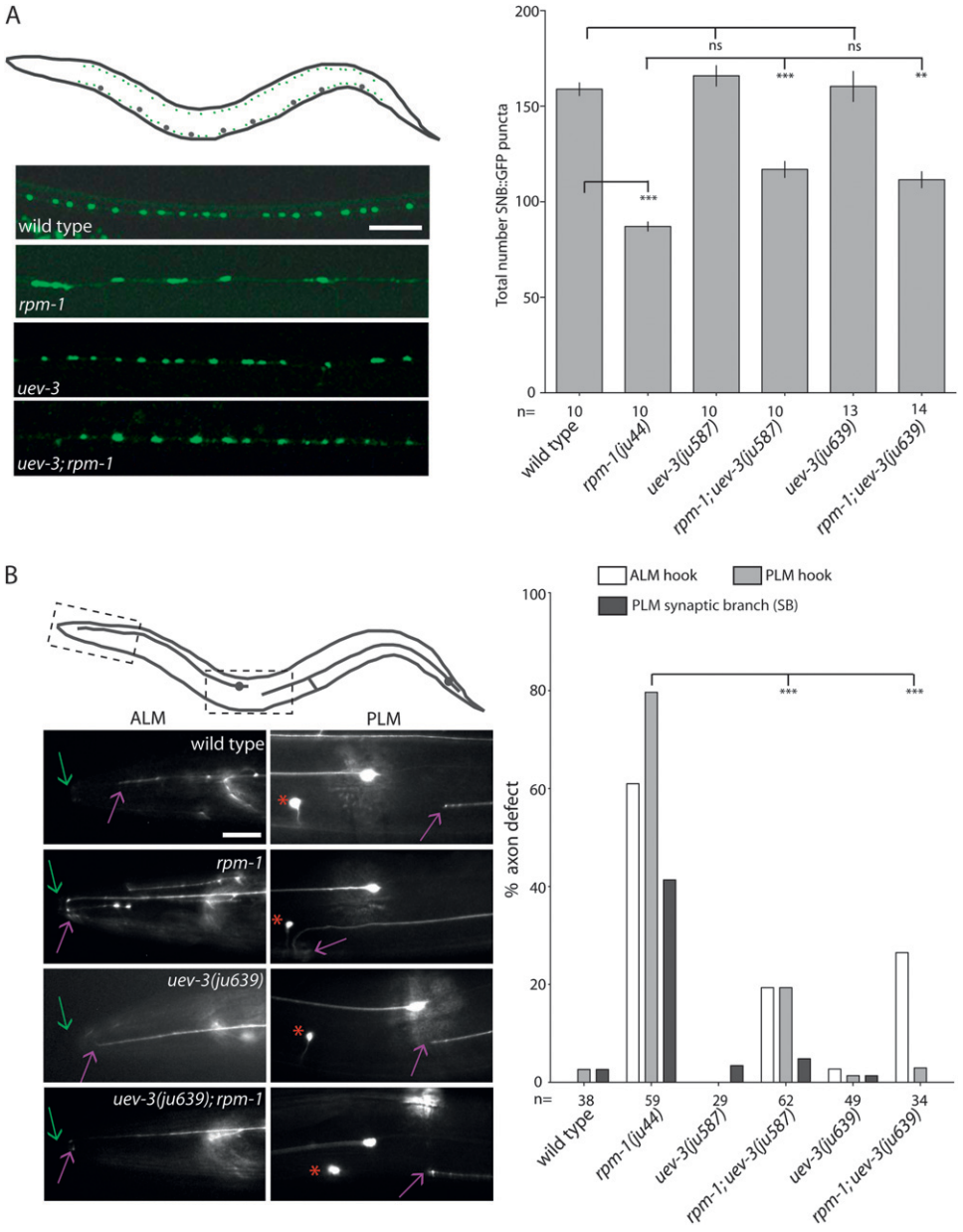

FIGURE 2.—*uev-3* suppresses *rpm-1* defects in motor neuron synapse formation and mechanosensory neuron axon termination. (A) Top left schematic of an animal expressing *Punc-25-SNB-1::GFP* (*juIs1*). Cell bodies (large gray dots) reside in the ventral cord, and synaptic SNB-1::GFP puncta (small green dots) reside along the ventral and dorsal cords. The epifluorescent images below show SNB-1::GFP in the dorsal cords in 1-day-old adult animals with genotypes as indicated. Scale bar, 10 μm. The graph on the right shows the quantification of SNB-1::GFP in the dorsal cord (mean ±SEM). *n* indicates number of animals scored. Statistics, ANOVA with Bonferroni correction: (**) $P < 0.01$; (***) $P < 0.001$; (ns) not significant. (B) Schematic of animal expressing *Pmec-7::GFP* (*muIs32*), marking one each of the bilaterally symmetric ALM and PLM neurons. Images below show portion of the ALM and PLM axons, corresponding to the dash-boxed regions. The tip of the animal's nose is indicated with green arrows, and ALM and PLM axon termination site is indicated with purple arrows. Red asterisks mark ALM cell body. ALM axon termination defects occur when the axon tip extends into the tip of the nose and loops back (or hook). PLM axon termination defects include absence of synapse branch or "hook" such that the PLM axon overextends beyond normal termination site and turns ventrally or turns ventrally before normal termination site. The graph shows the suppression of *rpm-1* by *uev-3* in three categories. *n* indicates animals scored. Statistics, Fischer exact test, comparing the PLM "hook" defects: (***) $P < 0.001$.

motif, which is important for proper folding of the active site region in UBC proteins, is conserved in UEV-3 (Figure S1) (GUDGEN *et al.* 2004). The overall sequence of UEV-3 is most similar to *C. elegans* UEV-2, followed by UBC-3 and UBC-7 in *C. elegans* (Figure 1C), and divergent from canonical UEVs (see below).

***uev-3(lf)* suppresses the defects in motor and mechanosensory neurons of *rpm-1(lf)*:** *rpm-1(lf)* mutants display irregularly shaped and sized presynaptic terminals in the motor neurons (ZHEN *et al.* 2000). The mutants also show axon termination defects in the mechanosensory neurons (SCHAEFER *et al.* 2000). Despite these defects, *rpm-1(lf)* animals appear superficially wild type in the overall nervous system architecture and locomotory behavior. The *uev-3* mutants alone also develop normally and exhibit no discernable abnormalities in the motor and mechanosensory neurons (Figure 2). However, in an *rpm-1(lf)* background, mutations in *uev-3* can ameliorate the defects in motor neuron synapses and touch axon patterning.

We determined the extent of *rpm-1(lf)* suppression by *uev-3(lf)*. We first analyzed the presynaptic puncta patterns and numbers using *juIs1 [Punc25-SNB-1::GFP]*, a marker that visualizes presynaptic terminals in GABA motor neurons (HALLAM and JIN 1998). In wild-type animals, this marker shows a pattern of uniformly sized and spaced fluorescent puncta along the dorsal and ventral cords, and on average, 158.9 puncta are visible in

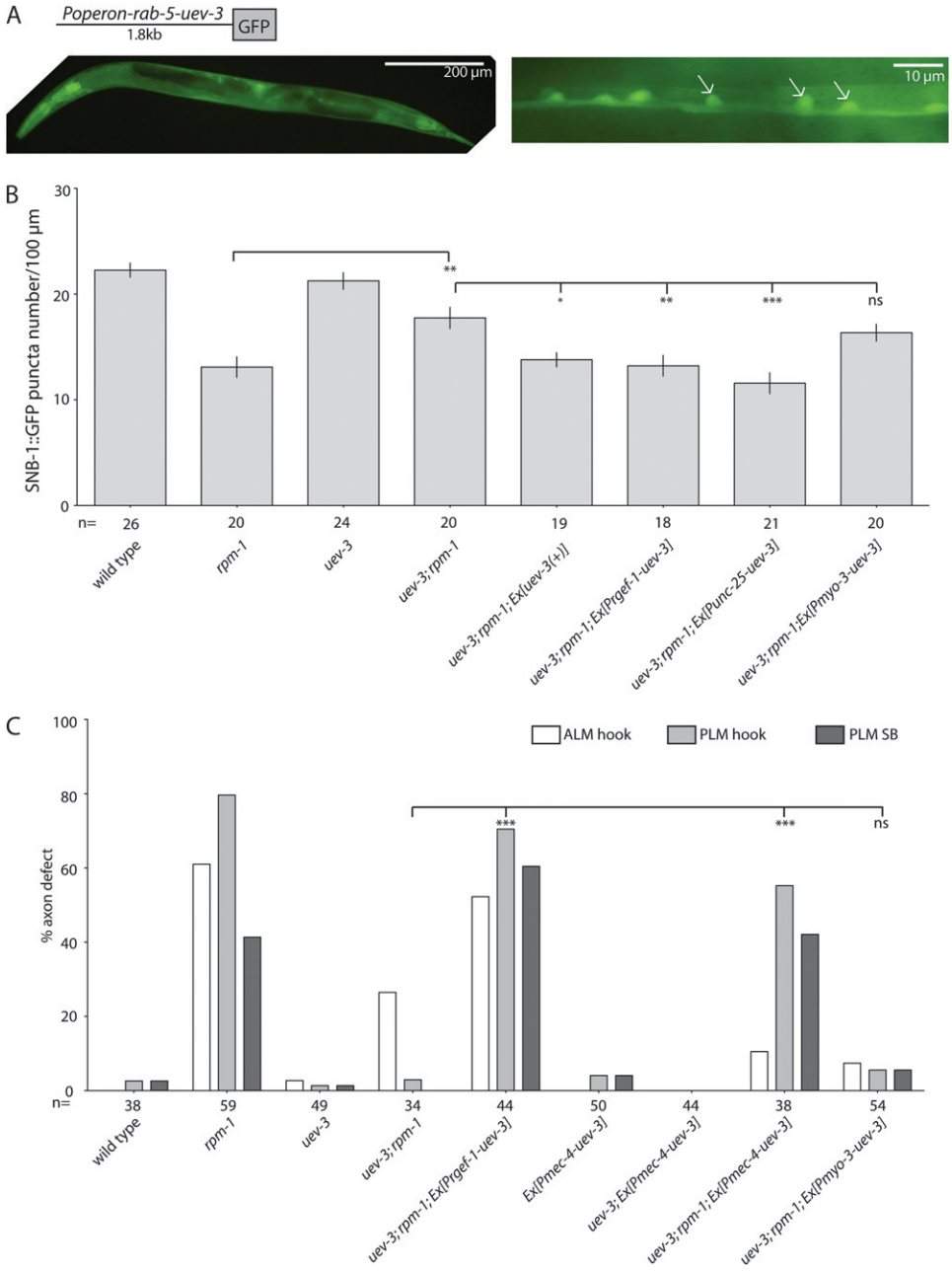

FIGURE 3.—UEV-3 functions cell autonomously in presynaptic neurons. (A) The 1.8-kb promoter of the operon driven GFP (*ixEx2 [Puev-3-GFP]*) expression in many tissues (left), including the motor neurons of the ventral cord (white arrows, right). (B) Presynaptic expression of UEV-3 rescues the suppression of *rpm-1* by *uev-3* in the GABAergic motor neurons. *Prgef-1*, 3.5-kb pan-neural promoter; *Punc-25*, 1.2-kb GABAergic motor neuron promoter, and *Pmyo-3*, 1-kb body muscle promoter. Quantification of SNB-1::GFP puncta in the dorsal nerve cord of young adults is shown as mean ± SEM; *n* as indicated. Statistics, ANOVA with Bonferroni correction: (*) $P < 0.05$, (**) $P < 0.01$, (***) $P < 0.001$, (ns) not significant. (C) Cell-autonomous rescue of the suppression of *rpm-1 by* uev-3 in touch neurons driven by the *Pmec-4* promoter. n indicates animals scored. Statistics, Fischer Exact Test, comparing the PLM "hook" defects: (***) $P < 0.001$, (ns) not significant.

the dorsal cord (Figure 2A). *rpm-1(lf)* mutants have fewer puncta, averaging 87.1 puncta in the dorsal cord. The remaining GFP puncta in *rpm-1* mutants are often enlarged and disorganized in distribution. Single mutants of *uev-3(ju587)* or *uev-3(ju639)* have an average 165.9 or 160.4 puncta per dorsal cord, respectively, and SNB-1::GFP puncta patterns are similar to wild type. Both *uev-3(ju587); rpm-1(lf)* and *uev-3(ju639); rpm-1(lf)* double mutants show significant suppression of the *rpm-1* phenotype, increasing SNB-1::GFP puncta number to an average of 116.9 and 111.6 in the dorsal cord, respectively.

We also examined the touch neuron morphology using the *muIs32* [*Pmec-7-GFP]* marker (CH'NG *et al.* 2003). In wild-type animals, the ALM cell body lies laterally in the midbody region and sends a longitudinal axonal projection anterior into the pharyngeal region of the animal where a process branches into the nerve ring and forms synapses (Figure 2B). The PLM cell body resides in the tail and sends a projection anterior into the midbody of the animal, terminating posterior to the ALM cell body. PLM cells also extend a synaptic branch to the ventral cord to form synapses onto its partners. In *rpm-1(lf)* mutants, both ALM and PLM axons frequently overextend beyond their normal termination sites and loop posteriorly or into the ventral cord, described as "ALM hook" or "PLM hook" defects, respectively (Figure 2B). Additionally, the PLM synaptic branch is frequently missing. Although low levels of ALM and PLM defects are detected in *uev-3(ju587)* and

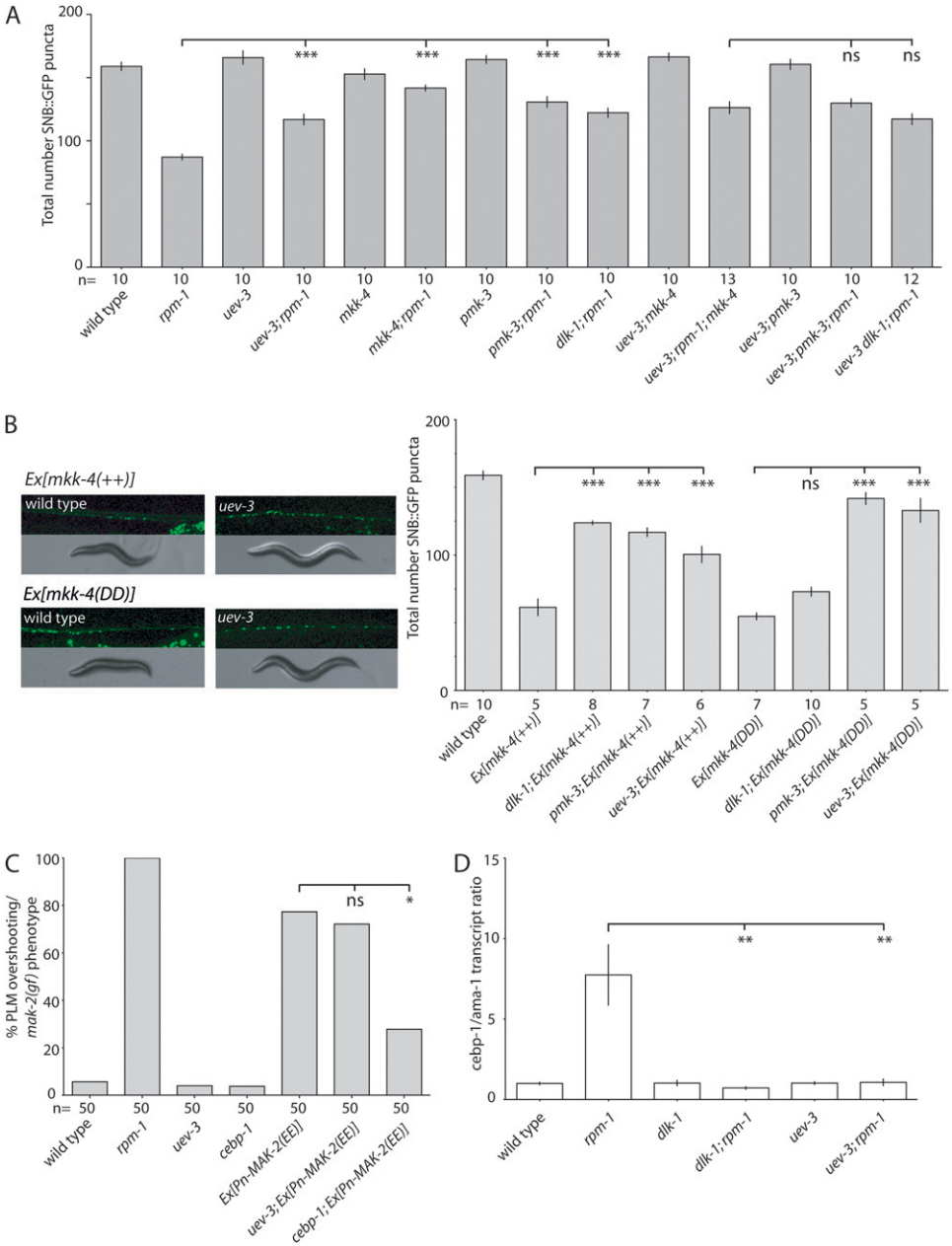

FIGURE 4.—*uev-3* acts in the DLK-1 MAPK cascade, downstream of *mkk-4*, and upstream of *mak-2*. (*) $P < 0.05$, (**) $P < 0.01$, (***) $P < 0.001$, (ns) not significant. (A) *uev-3(lf)* does not further enhance the suppression of *rpm-1* in the motor neuron synapses by *pmk-3* or *mkk-4* or *dlk-1*. Numbers are mean ± SEM, *n* as indicated. Statistics, ANOVA with Bonferroni correction compared with *rpm-1* single mutant. (B) *uev-3* functions downstream of *mkk-4* MAPKK. Transgenic animals overexpressing wild-type MKK-4 [*mkk-4(++), juEx490*] or expressing the constitutively active version of MKK-4 [*mkk-4(DD), juEx669*] display similarly abnormal synaptic patterns (*juIs1*), uncoordinated locomotion, and small body size (left). The phenotypes of both types of transgenes are suppressed by *uev-3(ju587),* and quantitation is shown on the right (mean ± SEM); ANOVA with Bonferroni correction: *n* as indicated. (C) *uev-3* acts upstream of *mak-2*. Expression of a phosphomimetic MAK-2(EE) causes gain-of-function effects, which is suppressed by *cebp-1*, but not by *uev-3*. n as indicated. Statistics, Fischer exact test. (D) *uev-3* acts in the *dlk-1* pathway to regulate levels of *cebp-1* transcripts, qRT–PCR levels of *cebp-1* mRNAs normalized against *ama-1*. Statistics, Student's t-test: $n = 3$.

uev-3(ju639) mutants, both mutations significantly suppressed *rpm-1(lf)* (Figure 2B). The degree of suppression of *rpm-1(lf)* by both alleles of *uev-3* is comparable to those observed for the mutants in the DLK-1 MAPK cascade (GRILL *et al.* 2007). *uev-3(ju639)* has a slightly stronger suppression effect on the mechanosensory neuron phenotypes, so we have designated *ju639* as the cannonical mutation of the gene.

***uev-3* acts cell autonomously in presynaptic neurons:** We determined the transcriptional expression pattern of the *rab-5* and *uev-3* operon using 1.8 kb of the 5′-upstream sequences of the operon to drive GFP expression. GFP is observed in all tissues and is noticeably present in ventral cord neurons (Figure 3A). We next addressed whether UEV-3 acts cell autonomously in neurons by expressing *uev-3* cDNA driven by tissue-specific promoters in *uev-3; rpm-1* mutants (Table S2 and Table S3). We examined functional rescue of the motor neuron synaptic phenotypes by quantitating SNB-1::GFP puncta numbers (Figure 3B). Expression of *uev-3* driven by a pan-neuronal promoter, or a motor neuron specific promoter rescues the suppression of *rpm-1(lf)* to similar degree comparable to that of transgenic-expressing *uev-3* genomic DNA. The muscle promoter driven transgene did not show any effects on the suppression in *uev-3; rpm-1* mutants. Similarly, we expressed *uev-3* cDNA in touch neurons, and observed significant rescue of the suppression on the mechanosensory neuron phenotypes (Figure 3C). As in motor neurons, the muscle-driven promoter did not show any

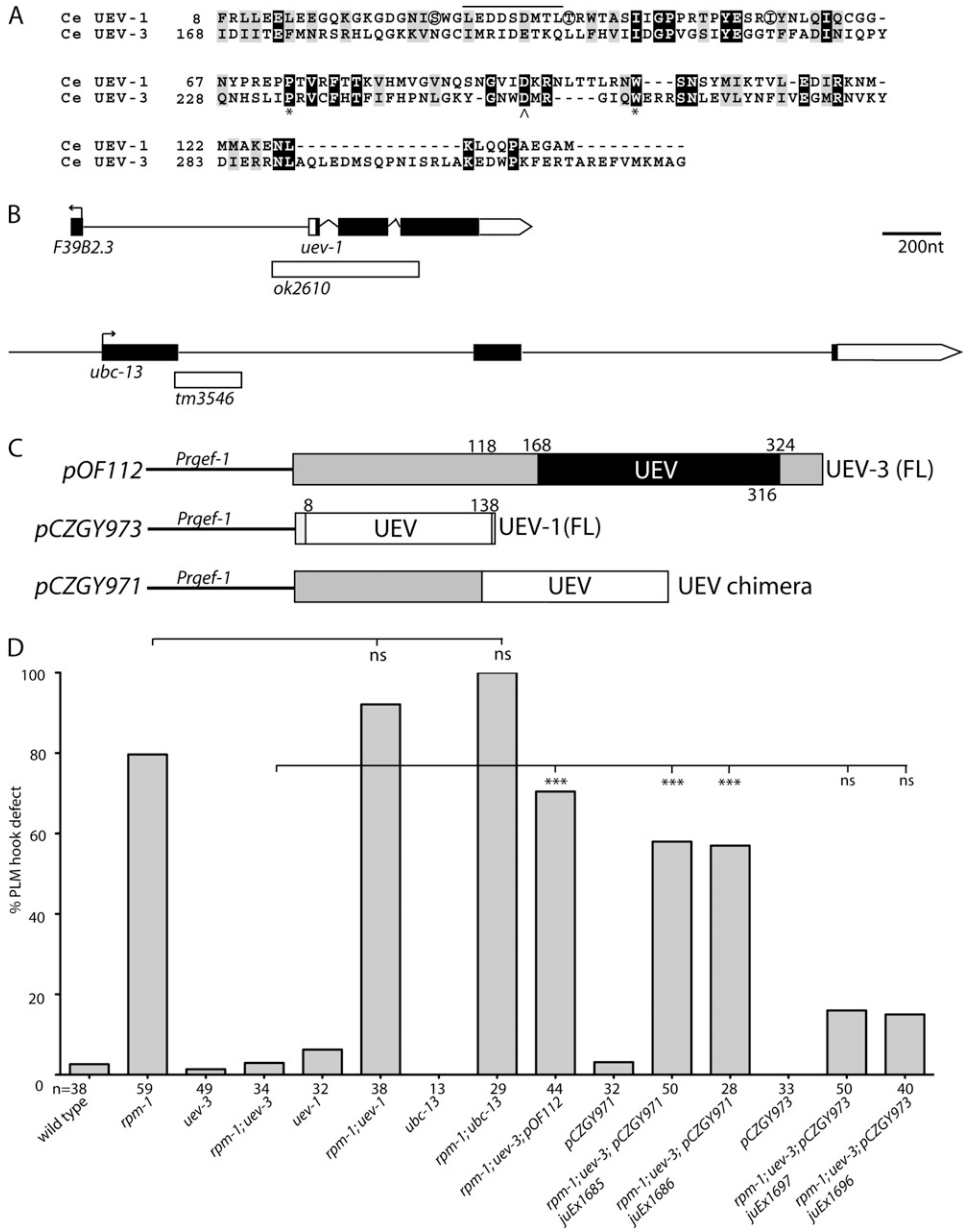

FIGURE 5.—Functional comparison of UEV-1/UBC-13 and UEV-3. (A) Alignment of UEV-1 and UEV-3 UEV domains. Black boxes, identical residues and gray boxes, similar residues. Asterisk, conserved proline and tryptophan residues; caret, aspartic acid residue at the position where both UEV proteins lack the active cysteine. Solid line above residues in UEV-1 31-39 indicates the conserved region that would be important for interacting with Ubc13. Circled Ser, Thr and Ile residues have been shown to be on the interface of *S. cerevisiae* Mms2 with ubiquitin, which are not conserved in UEV-3. (B) Illustration of the *uev-1* and *ubc-13* genes and mutations. (C) Schematics of DNA constructs used in transgenic lines in panel D. (D) Quantification of genetic interactions between *uev-1, ubc-13* and *rpm-1* and transgenic UEV expression. Statistics, Fischer Exact Test; (***) $P < 0.001$; (ns) not significant.

rescue activity in *uev-3; rpm-1* mutants. The transgenes alone or in a *uev-3* background did not cause any significant defects (Figure 3C, data not shown for *[Pmyo-3-uev-3]* and *[Prgef-1-uev-3]* transgenes alone). These results thus demonstrate that *uev-3* is required cell autonomously in presynaptic neurons.

***uev-3* acts downstream of *mkk-4* and upstream of *mak-2* in the DLK-1 MAPK cascade:** To learn how *uev-3* functions in the DLK-1 MAPK cascade, we performed four lines of experiments. First, we made pairwise loss-of-function mutant combinations between *uev-3* and the MAPK genes and measured the suppression of motor neuron puncta numbers in *rpm-1(lf)* (Figure 4A). For example, *uev-3; rpm-1* have 116.9 SNB-1::GFP puncta per dorsal cord, and *pmk-3; rpm-1* have 130.7 puncta per dorsal cord. The triple mutants *uev-3; pmk-3; rpm-1* show a mean 129.9 puncta number in the dorsal cord and do not suppress *rpm-1* any stronger than either double mutants. This analysis is consistent with the interpretation that *uev-3* acts in the same pathway with MAPK genes *dlk-1, mkk-4,* and *pmk-3*.

Second, to place *uev-3* within the DLK-1 MAPK pathway, we took advantage of the observations that transgenic expression of either wild type *mkk-4(++)* or a phosphomimetic *mkk-4(DD)* in a wild-type background causes gain-of-function phenotypes (NAKATA *et al.* 2005). The animals carrying these extra-chromosomal arrays display an uncoordinated movement, with disorganized synaptic puncta resembling those of *rpm-1(lf)* (Figure 4B). Loss-of-function in *pmk-3*, a gene downstream of *mkk-4,* can suppress both the synaptic and behavior defects associated with either *mkk-4(++)* or *mkk-4(DD)* transgene, whereas loss-of-function in *dlk-1,* which acts upstream of *mkk-4,* only suppresses the

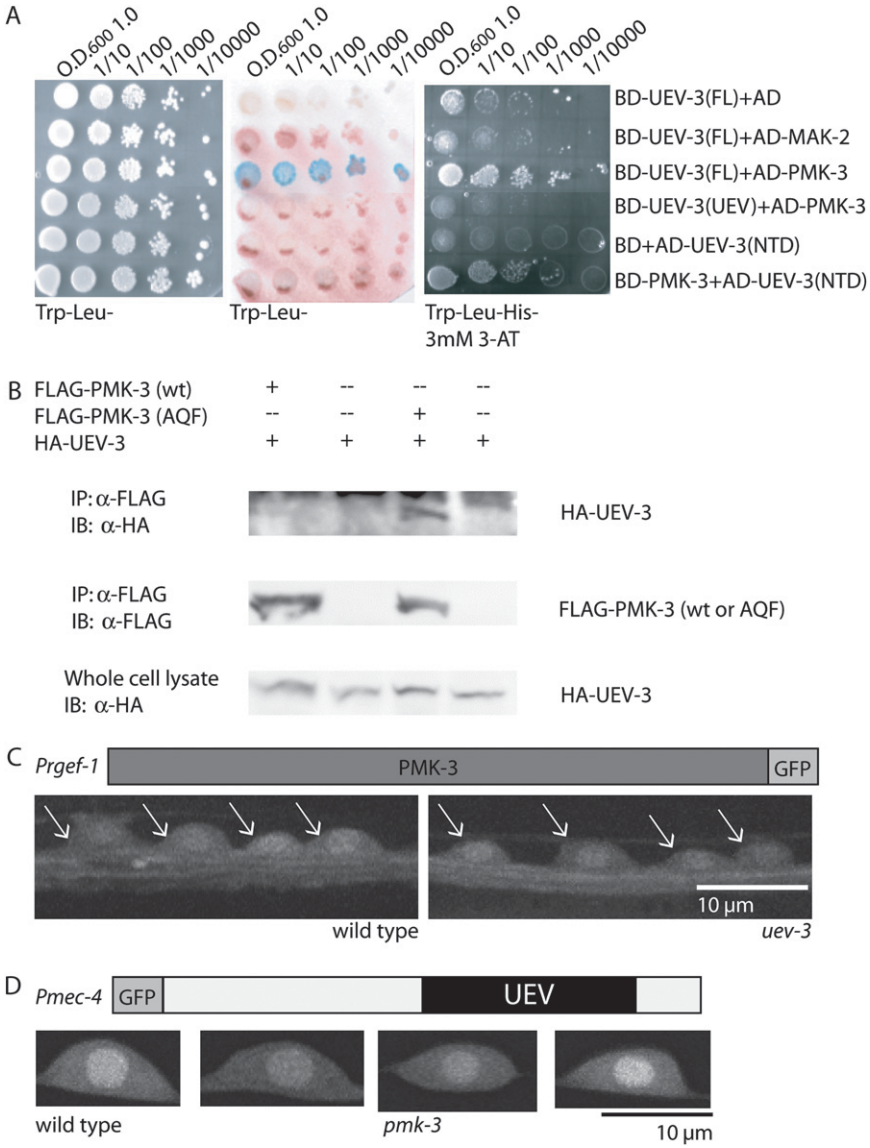

FIGURE 6.—UEV-3 likely binds PMK-3. (A) UEV-3 interacts with PMK-3 but not with MAK-2 in yeast two-hybrid interaction assay, Trp–Leu plates (left), lacZ assay (middle), and Trp–Leu–His plates containing 3 mM 3-AT (right). UEV-3(FL), full-length UEV-3; UEV-3(UEV), UEV domain only; UEV-3(NTD), N-terminal domain, BD is binding domain and AD is activating domain. (B) HA-UEV-3 coimmunoprecipitated with FLAG-PMK-3(AQF) mutant but not with FLAG-PMK-3 wild type when coexpressed in 293T cells. (C) Functional PMK-3::GFP (*juEx675 [Prgef-1-PMK-3::GFP]*) in neurons is seen in cytoplasmic and nuclear compartments in wild type and is unaltered in *uev-3(ju587)* background. Arrows indicate neurons in the ventral cord. (D) Functional UEV-3::GFP in mechanosensory neurons *[juEx2118 Pmec-4-GFP::UEV-3]* localizes to cytoplasm and nucleus and is unaltered in *pmk-3* mutant background.

effects of *mkk-4(++)* (NAKATA *et al.* 2005). We found that when either the *mkk-4(++)* or *mkk-4(DD)* transgene is in the *uev-3(lf)* background, the body size and movement phenotypes of the transgenic animals are abolished, and the average total synaptic GFP puncta are increased significantly (Figure 4B). Thus, *uev-3* behaves genetically similar to *pmk-3* and likely acts downstream of *mkk-4*.

Third, we have recently identified that the MAP kinase-activated protein kinase MAK-2 and the transcription factor CEBP-1 function downstream of PMK-3 (YAN *et al.* 2009). Transgenic overexpression of a phosphomimetic MAK-2, *mak-2(EE)*, causes a gain-of-function defect resembling *mkk-4(gf)* transgenes, which are suppressed by loss-of-function in *cebp-1* but not *pmk-3* (YAN *et al.* 2009) (Figure 4C). We found that *uev-3(lf)* does not suppress the *mak-2(EE)* gain-of-function defects (Figure 4C), consistent with a conclusion that *uev-3* likely acts upstream of *mak-2*.

Finally, we examined the levels of *cebp-1* mRNA transcripts in *uev-3* mutants. The DLK-1 MAP kinase cascade regulates *cebp-1* by controlling the levels of *cebp-1* mRNA (YAN *et al.* 2009). We performed quantitative RT–PCR on RNAs isolated from mixed-stage animals and compared the levels of *cebp-1* transcripts to those of *ama-1*, the large subunit of RNA polymerase II (SANFORD *et al.* 1983). In *rpm-1* mutants, *cebp-1* transcript levels are elevated compared to wild type because DLK-1 is not degraded, allowing high-level of MAP kinase signaling to promote the stability of *cebp-1* mRNA (Figure 4D). In both *rpm-1; dlk-1* and *rpm-1; uev-3* mutant strains, the transcript levels of *cebp-1* are comparable to wild-type levels. All together, these four lines of evidence show that *uev-3* functions in the DLK-1 MAPK pathway, at the step between *mkk-4* and *mak-2*.

The canonical *uev-1* and *ubc-13* do not suppress *rpm-1*: Biochemical studies of canonical UEV proteins in yeast and mammalian cells, such as Mms2 and Uev1A,

respectively, have established that the UEV domain functions as an obligatory subunit for an active Ubc, Ubc13 (Broomfield *et al.* 1998; Xiao *et al.* 1998; Deng *et al.* 2000). The Uev1A/Ubc13 E2 complex catalyzes Lys63 poly-ubiquitin chain formation (Hofmann and Pickart 1999; Vandemark *et al.* 2001). The ortholog of Mms2 or Uev1A in *C. elegans* is UEV-1, which can interact with UBC-13 (Gudgen *et al.* 2004). The UEV domain of the UEV-3 is very divergent from the canonical UEV (Figure 1C and Figure S1) and also shows limited degree of similarities to that of UEV-1 (14.7% identity and 30.6% similarity) (Figure 5A). Residues known to be important for Uev1 binding to either its cognate Ubc13 or ubiquitin do not seem to be conserved in UEV-3 (Moraes *et al.* 2001; Vandemark *et al.* 2001) (Figure 5A). In addition, UEV-3 has extended N-terminal sequences and short C-terminal tail (Figure 5B). The sequence comparisons raise the question whether UEV-3 may retain functions similar to those of UEV proteins in other organisms.

We tested whether *uev-1* and *ubc-13* interacted with *rpm-1*. The *uev-1* gene is a small gene, with its coding sequences less than 1 kb, and resides in an operon as the upstream gene (Figure 5B). A deletion allele, *ok2610*, removes 496 bp starting 142 bp in the promoter of the operon and ending 69 bp in the third exon of *uev-1*, and is likely a null mutation. The homozygous *ok2610* animals are viable, develop normal touch neurons, and do not suppress *rpm-1(lf)* (Figure 5D). We also examined a deletion allele of *ubc-13*, *tm3546*, which breaks in the first exon and would lead to a premature stop at amino acid 88 (Figure 5B). We observed no genetic suppression of *rpm-1(lf)* by *ubc-13(tm3546)* (Figure 5D). Moreover, overexpression of *uev-1* did not bypass the requirement of *uev-3* (Figure 5D). We also made a chimeric gene in which we replaced the UEV domain and C terminus of UEV-3 with the UEV domain from UEV-1 (Figure 5C). Intriguingly, we found that transgenic expression of this UEV chimeric protein in neurons rescued the suppression of *rpm-1(lf)* in the *uev-3; rpm-1* background to similar levels as does the expression of the full-length *uev-3* (Figure 5D). With the caveat of overexpression, this result suggests that despite its divergency, the UEV domain of UEV-3 could have a function similar to that of the canonical UEV domain of UEV-1. We therefore wanted to test whether UEV-3 might require any other UBC. *C. elegans* has 22 annotated UBC genes. We analyzed available deletion or mutant alleles for several UBC genes, but observed no genetic interactions with *rpm-1(lf)* (Table S1). We also performed dsRNAi for 19 *ubc* genes in *eri-1; rpm-1; muIs32* strain and did not observe detectable suppression of *rpm-1(lf)* (data not shown). We also tested protein interactions between UEV-3 and UBC genes using yeast two-hybrid assays and were not able to detect a positive interaction with UEV-3, out of 11 UBC genes and 2 UEV genes tested (data not shown). In summary, these studies suggest a scenario in which the UEV domain of UEV-3 might have a canonical function like UEV-1, but UEV-3 might likely have distinct partners for its function.

UEV-3 can bind PMK-3: To better characterize the relationship between UEV-3 and the DLK-1 MAPK cascade, we asked whether UEV-3 could interact with the kinases by performing yeast two-hybrid assays between UEV-3 and all four kinases and CEBP-1. We detected interactions between UEV-3 and PMK-3, but not between UEV-3 and the other three kinases or CEBP-1 (Figure 6A, data not shown for *dlk-1, mkk-4, cebp-1*). We attempted to narrow down the interacting domains using bait expressing only the UEV domain or N-terminal domain of UEV-3, but were hindered by self-activation of the N-terminal expression construct and were not able to observe strong interactions between either domain alone and PMK-3 (Figure 6A). We further tested the binding interactions between UEV-3 and PMK-3 by co-immunoprecipitation studies in heterologous 293T cells. Although wild-type PMK-3 was not detectable in the immunocomplex with UEV-3, we observed co-immunoprecipitation between UEV-3 and a mutant PMK-3 in which the catalytic active site was mutated (Figure 6B). Such catalytic active site mutants of MAP kinases are often used to detect transient interactions between MAP kinases and their substrates or interacting partners (Han *et al.* 1997). Finally, we asked if this protein interaction might play roles in the localization or abundance of each protein. We generated transgenic animals expressing functional PMK-3::GFP or UEV-3::GFP in neurons. Both tagged proteins show ubiquitous expression in cytosol and nucleus (Figure 6, C and D). When each transgene was crossed into *pmk-3* or *uev-3* mutants, we did not observe major differences in the localization pattern or expression level of either transgene. Moreover, overexpression of *pmk-3(+)* in *uev-3*; *rpm-1* mutants does not cause any detectable effects, nor does the overexpression of *uev-3(+)* in *pmk-3; rpm-1* mutants (data not shown). Together with the genetic epistasis analyses, these data suggest that UEV-3 and PMK-3 are likely functional partners.

DISCUSSION

The conserved DLK kinases have recently emerged as key regulators of axon and synapse development in the nervous systems of both vertebrates and invertebrates (Po *et al.* 2010). The mechanistic dissection of the DLK signal transduction cascade has only just begun. In this study, we identified and characterized a new member of the DLK-1 kinase pathway, UEV-3, a previously uncharacterized ubiquitin-conjugating enzyme/E2 variant. Like other MAPKs known to function in the DLK-1 pathway, loss-of-function of *uev-3* on its own is grossly wild type, but shows specific suppression of *rpm-1* in

axon termination and synapse formation phenotypes. Our genetic epistasis studies reveal that *uev-3* acts in the DLK-1 MAPK pathway, downstream of *mkk-4* and upstream of *mak-2*. On the basis of our studies of UEV-3 protein and its tentative binding interactions with PMK-3, we propose that UEV-3 may act as a cofactor for PMK-3, for example, to modulate PMK-3 activation or to recognize substrates, resulting in fine tuning the DLK-1 signal transduction cascade.

A ubiquitin-conjugating enzyme variant could provide an additional means for pathway regulation and specificity by delineating the targets of the pathway. The UEV protein, Fts1, has been shown to act as a scaffold between protein kinase B (PKB/Akt) and 3-phosphoinositide-dependent kinase 1 (PDK1) (Remy and Michnick 2004). *C. elegans* has three closely related p38 MAP kinases that appear to be ubiquitously expressed (Berman *et al.* 2001). The function of UEV-3 may be to provide specificity for PMK-3 in the DLK-1 MAPK pathway during synaptogenesis and axon termination in neurons. Through the UEV-3 and PMK-3 interaction, substrates important for these processes may be selectively activated. Despite substantial efforts, we have not yet been able to directly test the contribution of UEV-3 in the activation of MAK-2, because of the lack of reagents to detect phosphorylated MAK-2 *in vivo*. However, the idea that UEV-3 could help PMK-3 to affect kinase activation, such as that of MAK-2, would be similar to those revealed by the role of Uev1/Ubc13 in TAK1 kinase activation in the IkK pathway (Deng *et al.* 2000; Wang *et al.* 2001).

Defining the roles of proteins linked to ubiquitination in the nervous system has been a major advance in the past decade (Tai and Schuman 2008). Comparing to what we have learned about the E3 ubiquitin ligases, relatively little is understood about the functional specificity and regulation of E2 enzymes. A classic example is the Drosophila Bendless (Thomas and Wyman 1984; Muralidhar and Thomas 1993), which is implicated in synapse function but acts distinctly different from the E3 ligase Highwire (Uthaman *et al.* 2008). Emerging expression studies suggest that UEV proteins are widely expressed in the developing nervous system (Watanabe *et al.* 2007). However, their functions are largely unknown. Our transgenic studies suggest that despite the sequence divergency of the UEV domain, UEV-3 might act in a manner similar to canonical UEV proteins. Nonetheless, with the limitations of available reagents, we were not able to identify a cognate E2 ubiquitin-conjugating enzyme for UEV-3.

An intriguing possibility remains that UEV-3 may be functioning on its own to help add additional regulation in the RPM-1 pathway. It is well established that the UEV protein Tsg101/Vps23 acts in the endocytic pathway to bind ubiquitinated proteins and remove them from the membrane (Katzmann *et al.* 2002). The endosomal sorting complex required for transport (ESCRT-1) contains Vps23 and two other Vps proteins necessary for recognizing and sorting cargo endocytosed at the plasma membrane. Vps23 binds ubiquitin conjugated to proteins at the plasma membrane and together with the ESCRT-II and -III complexes, target proteins are sorted through multivesicular bodies in the endosomal pathway. A recent study has shown that a splice variant of human Uev1 has an extended N-terminal domain, which can target the protein to endosomal-like organelles and confer regulation to EGF receptor signaling, possibly through protein degradation (Duex *et al.* 2010). UEV-3 is unusual in that it has a long N-terminal extension, which could have a regulatory role in UEV-3 function. This idea would be consistent with the observation that overexpression of the chimeric UEV-3-UEV-1 mimics the activity of full-length UEV-3, whereas overexpression of UEV-1 does not. The RPM-1 pathway has previously been connected to vesicular regulation through the biochemical interaction between RPM-1 and the RabGEF GLO-4 (Grill *et al.* 2007). A tempting possibility is that UEV-3 may provide crosstalk between the GLO-4 and DLK-1 pathways by binding ubiquitinated proteins through its UEV domain and acting in the endosomal pathway. Potential future directions would be to identify UEV-3-interacting proteins to aid in further elucidation of UEV-3′s mechanism in axon termination and synapse formation.

We thank H. Taru for advice on Yeast two-hybrid, L. Boyd for *C. elegans* Ubc clones, and our lab members for input. We are grateful for the deletion alleles generated by Shohei Mitani and the National Bioresearch Project (Tokyo Women's Medical University School of Medicine, Tokyo, Japan) and *C. elegans* knockout consortium. Some of the strains were obtained from *Caenorhabditis* Genetics Center, which is supported by grants from National Institutes of Health (NIH)–National Center for Research Resources. This work was supported by Japan's Grant-in-Aid for Scientific Research (19500306) to K.N., NIH R01-035546 to Y.J. D.Y. is a research associate and Y.J. an investigator of the Howard Hughes Medical Institute.

LITERATURE CITED

Babst, M., G. Odorizzi, E. J. Estepa and S. D. Emr, 2000 Mammalian tumor susceptibility gene 101 (TSG101) and the yeast homologue, Vps23p, both function in late endosomal trafficking. Traffic **1:** 248–258.

Berman, K., J. McKay, L. Avery and M. Cobb, 2001 Isolation and characterization of pmk-(1–3): three p38 homologs in *Caenorhabditis elegans*. Mol. Cell. Biol. Res. Commun. **4:** 337–344.

Bloom, A. J., B. R. Miller, J. R. Sanes and A. DiAntonio, 2007 The requirement for Phr1 in CNS axon tract formation reveals the corticostriatal boundary as a choice point for cortical axons. Genes Dev. **21:** 2593–2606.

Brenner, S., 1974 The genetics of *Caenorhabditis elegans*. Genetics **77:** 71–94.

Broomfield, S., B. L. Chow and W. Xiao, 1998 MMS2, encoding a ubiquitin-conjugating-enzyme-like protein, is a member of the yeast error-free postreplication repair pathway. Proc. Natl. Acad. Sci. USA **95:** 5678–5683.

Ch'ng, Q., L. Williams, Y. S. Lie, M. Sym, J. Whangbo *et al.*, 2003 Identification of genes that regulate a left-right asymmetric neuronal migration in *Caenorhabditis elegans*. Genetics **164:** 1355–1367.

Collins, C. A., Y. P. Wairkar, S. L. Johnson and A. Diantonio, 2006 Highwire restrains synaptic growth by attenuating a MAP kinase signal. Neuron **51:** 57–69.

Davis, M. W., M. Hammarlund, T. Harrach, P. Hullett, S. Olsen *et al.*, 2005 Rapid single nucleotide polymorphism mapping in *C. elegans*. BMC Genomics **6:** 118.

Deng, L., C. Wang, E. Spencer, L. Yang, A. Braun *et al.*, 2000 Activation of the IkappaB kinase complex by TRAF6 requires a dimeric ubiquitin-conjugating enzyme complex and a unique polyubiquitin chain. Cell **103:** 351–361.

DiAntonio, A., A. P. Haghighi, S. L. Portman, J. D. Lee, A. M. Amaranto *et al.*, 2001 Ubiquitination-dependent mechanisms regulate synaptic growth and function. Nature **412:** 449–452.

D'Souza, J., M. Hendricks, S. Le Guyader, S. Subburaju, B. Grunewald *et al.*, 2005 Formation of the retinotectal projection requires Esrom, an ortholog of PAM (protein associated with Myc). Development **132:** 247–256.

Duex, J. E., M. R. Mullins and A. Sorkin, 2010 Recruitment of Uev1B to Hrs-containing endosomes and its effect on endosomal trafficking. Exp. Cell Res.

Fields, S., and R. Sternglanz, 1994 The two-hybrid system: an assay for protein-protein interactions. Trends Genet. **10:** 286–292.

Grill, B., W. V. Bienvenut, H. M. Brown, B. D. Ackley, M. Quadroni *et al.*, 2007 C. elegans RPM-1 Regulates Axon Termination and Synaptogenesis through the Rab GEF GLO-4 and the Rab GTPase GLO-1. Neuron **55:** 587–601.

Gudgen, M., A. Chandrasekaran, T. Frazier and L. Boyd, 2004 Interactions within the ubiquitin pathway of *Caenorhabditis elegans*. Biochem. Biophys. Res. Commun. **325:** 479–486.

Hallam, S. J., and Y. Jin, 1998 lin-14 regulates the timing of synaptic remodelling in *Caenorhabditis elegans*. Nature **395:** 78–82.

Han, J., Y. Jiang, Z. Li, V. V. Kravchenko and R. J. Ulevitch, 1997 Activation of the transcription factor MEF2C by the MAP kinase p38 in inflammation. Nature **386:** 296–299.

Hofmann, R. M., and C. M. Pickart, 1999 Noncanonical MMS2-encoded ubiquitin-conjugating enzyme functions in assembly of novel polyubiquitin chains for DNA repair. Cell **96:** 645–653.

Hurley, J. H., S. Lee and G. Prag, 2006 Ubiquitin-binding domains. Biochem. J. **399:** 361–372.

Jin, Y., and C. C. Garner, 2008 Molecular mechanisms of presynaptic differentiation. Annu. Rev. Cell. Dev. Biol. **24:** 237–262.

Jones, D., E. Crowe, T. A. Stevens and E. P. Candido, 2002 Functional and phylogenetic analysis of the ubiquitylation system in *Caenorhabditis elegans*: ubiquitin-conjugating enzymes, ubiquitin-activating enzymes, and ubiquitin-like proteins. Genome Biol. **3:** research0002.

Katzmann, D. J., G. Odorizzi and S. D. Emr, 2002 Receptor downregulation and multivesicular-body sorting. Nat. Rev. Mol. Cell Biol. **3:** 893–905.

Kipreos, E. T., 2005 Ubiquitin-mediated pathways in *C. elegans* (December 01, 2005), *WormBook*, ed. The *C. elegans* Research Community, WormBook, doi/10.1895/wormbook.1.36.1, http://www.wormbook.org.

Lewcock, J. W., N. Genoud, K. Lettieri and S. L. Pfaff, 2007 The ubiquitin ligase Phr1 regulates axon outgrowth through modulation of microtubule dynamics. Neuron **56:** 604–620.

Li, H., G. Kulkarni and W. G. Wadsworth, 2008 RPM-1, a *Caenorhabditis elegans* protein that functions in presynaptic differentiation, negatively regulates axon outgrowth by controlling SAX-3/robo and UNC-5/UNC5 activity. J. Neurosci. **28:** 3595–3603.

Liao, E. H., W. Hung, B. Abrams and M. Zhen, 2004 An SCF-like ubiquitin ligase complex that controls presynaptic differentiation. Nature **430:** 345–350.

Mello, C. C., J. M. Kramer, D. Stinchcomb and V. Ambros, 1991 Efficient gene transfer in *C. elegans*: extrachromosomal maintenance and integration of transforming sequences. EMBO J. **10:** 3959–3970.

Moraes, T. F., R. A. Edwards, S. McKenna, L. Pastushok, W. Xiao *et al.*, 2001 Crystal structure of the human ubiquitin conjugating enzyme complex, hMms2-hUbc13. Nat. Struct. Biol. **8:** 669–673.

Muralidhar, M. G., and J. B. Thomas, 1993 The Drosophila bendless gene encodes a neural protein related to ubiquitin-conjugating enzymes. Neuron **11:** 253–266.

Nakata, K., B. Abrams, B. Grill, A. Goncharov, X. Huang *et al.*, 2005 Regulation of a DLK-1 and p38 MAP kinase pathway by the ubiquitin ligase RPM-1 is required for presynaptic development. Cell **120:** 407–420.

Pickart, C. M., and M. J. Eddins, 2004 Ubiquitin: structures, functions, mechanisms. Biochim. Biophys. Acta **1695:** 55–72.

Po, M. D., C. Hwang and M. Zhen, 2010 PHRs: bridging axon guidance, outgrowth and synapse development. Curr. Opin. Neurobiol. **20:** 100–107.

Raman, M., W. Chen and M. H. Cobb, 2007 Differential regulation and properties of MAPKs. Oncogene **26:** 3100–3112.

Remy, I., and S. W. Michnick, 2004 Regulation of apoptosis by the Ft1 protein, a new modulator of protein kinase B/Akt. Mol. Cell. Biol. **24:** 1493–1504.

Sancho, E., M. R. Vila, L. Sanchez-Pulido, J. J. Lozano, R. Paciucci *et al.*, 1998 Role of UEV-1, an inactive variant of the E2 ubiquitin-conjugating enzymes, in in vitro differentiation and cell cycle behavior of HT-29–M6 intestinal mucosecretory cells. Mol. Cell. Biol. **18:** 576–589.

Sanford, T., M. Golomb and D. L. Riddle, 1983 RNA polymerase II from wild type and alpha-amanitin-resistant strains of *Caenorhabditis elegans*. J. Biol. Chem. **258:** 12804–12809.

Schaefer, A. M., G. D. Hadwiger and M. L. Nonet, 2000 rpm-1, a conserved neuronal gene that regulates targeting and synaptogenesis in *C. elegans*. Neuron **26:** 345–356.

Skaug, B., X. Jiang and Z. J. Chen, 2009 The role of ubiquitin in NF-kappaB regulatory pathways. Annu. Rev. Biochem. **78:** 769–796.

Tai, H. C., and E. M. Schuman, 2008 Ubiquitin, the proteasome and protein degradation in neuronal function and dysfunction. Nat. Rev. Neurosci. **9:** 826–838.

Thomas, J. B., and R. J. Wyman, 1984 Mutations altering synaptic connectivity between identified neurons in Drosophila. J. Neurosci. **4:** 530–538.

Uthaman, S. B., T. A. Godenschwege and R. K. Murphey, 2008 A mechanism distinct from highwire for the Drosophila ubiquitin conjugase bendless in synaptic growth and maturation. J. Neurosci. **28:** 8615–8623.

VanDemark, A. P., R. M. Hofmann, C. Tsui, C. M. Pickart and C. Wolberger, 2001 Molecular insights into polyubiquitin chain assembly: crystal structure of the Mms2/Ubc13 heterodimer. Cell **105:** 711–720.

Wan, H. I., A. DiAntonio, R. D. Fetter, K. Bergstrom, R. Strauss *et al.*, 2000 Highwire regulates synaptic growth in Drosophila. Neuron **26:** 313–329.

Wang, C., L. Deng, M. Hong, G. R. Akkaraju, J. Inoue *et al.*, 2001 TAK1 is a ubiquitin-dependent kinase of MKK and IKK. Nature **412:** 346–351.

Watanabe, M., H. Mizusawa and H. Takahashi, 2007 Developmental regulation of rat Ubc13 and Uev1B genes in the nervous system. Gene Expr. Patterns **7:** 614–619.

Whitmarsh, A. J., 2006 The JIP family of MAPK scaffold proteins. Biochem. Soc. Trans. **34:** 828–832.

Wu, C., R. W. Daniels and A. DiAntonio, 2007 DFsn collaborates with Highwire to down-regulate the Wallenda/DLK kinase and restrain synaptic terminal growth. Neural Dev. **2:** 16.

Xiao, W., S. L. Lin, S. Broomfield, B. L. Chow and Y. F. Wei, 1998 The products of the yeast MMS2 and two human homologs (hMMS2 and CROC-1) define a structurally and functionally conserved Ubc-like protein family. Nucleic Acids Res. **26:** 3908–3914.

Yan, D., Z. Wu, A. D. Chisholm and Y. Jin, 2009 The DLK-1 kinase promotes mRNA stability and local translation in *C. elegans* synapses and axon regeneration. Cell **138:** 1005–1018.

Zhen, M., X. Huang, B. Bamber and Y. Jin, 2000 Regulation of presynaptic terminal organization by *C. elegans* RPM-1, a putative guanine nucleotide exchanger with a RING-H2 finger domain. Neuron **26:** 331–343.

Communicating editor: D. I. Greenstein

GENETICS

Supporting Information
http://www.genetics.org/cgi/content/full/genetics.110.117341/DC1

A Ubiquitin E2 Variant Protein Acts in Axon Termination and Synaptogenesis in *Caenorhabditis elegans*

Gloriana Trujillo, Katsunori Nakata, Dong Yan, Ichi N. Maruyama and Yishi Jin

DOI: 10.1534/genetics.110.117341

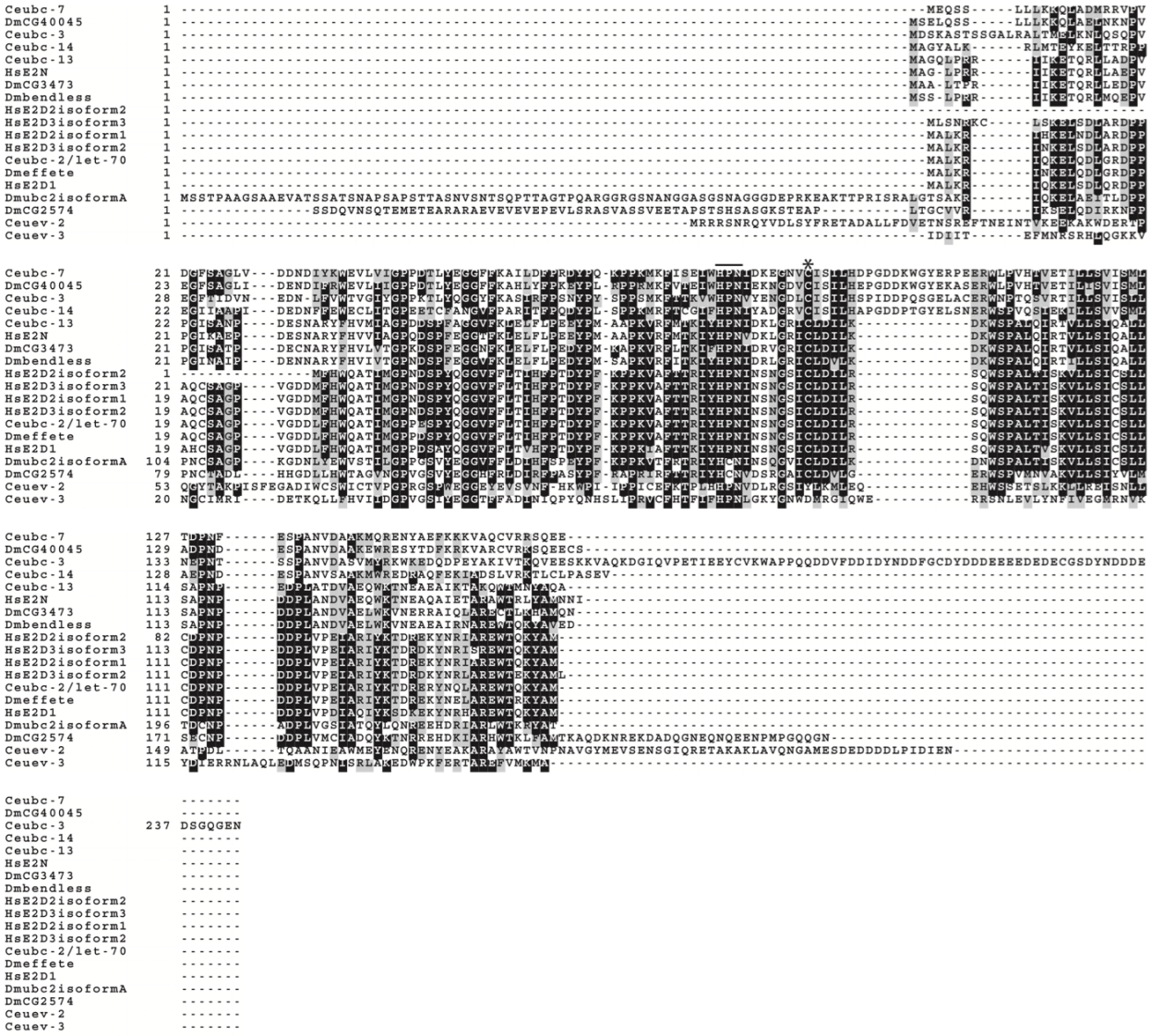

FIGURE S1.—Sequence alignment surrounding the active region in Ubc proteins showing homology between *H. sapiens*, *C. elegans*, and *D. melanogaster* from C. Exact matches are shaded in black, similar residues are shaded in grey. Asterisk denotes where UEV-3 lacks the critical cysteine residue. The Ubc folding motif, HPN/HCN, is noted by an underline.

TABLE S1

Summary of *ubc* and *uev* mutant alleles

Gene (allele)	Mutation	Primer sequence & detection method	Interaction with *rpm-1*
ubc-13(tm3546)	234 bp deletion, 17 bp insertion at the end of exon 1	YJ5577 cgattctccatttgctggtgg YJ5578 gatttggagccgaaagaagagc YJ 5580 ggggaaaatctattcacccttgag	does not suppress
ubc-16(ok3176)	684 bp deletion and 4bp insertion at end of exon 3 through 3'UTR	YJ5892 atgctgaatttgggtcccg YJ5893 gattccggatgataatcagaaattgataggc YJ5894 ttcggcgggagaacatagc	does not suppress
ubc-16(ok3177)	551 bp deletion and 35 bp insertion, creates a new stop codon and results in inappropriate gene length	YJ5892 atgctgaatttgggtcccg YJ5893 gattccggatgataatcagaaattgataggc YJ5894 ttcggcgggagaacatagc	does not suppress
ubc-24(ok3451)	~600 bp deletion from part of intron 1 to intron 4	YJ5886 caaggatgaaaggaatttggaa YJ5887 tgaatgtgcaaaaacccaaa YJ5895 gagaattggaaaccggagacc	does not suppress
ubc-25(ok1732)	1243 bp deletion from end of exon 2 through 3' UTR	YJ4845 aatcagaagaggatggcgtg YJ4846 agagccgagacagctgagag	does not suppress
uev-1(ok2610)	496 bp deletion from promoter through part of exon 3	YJ5022 acggatttattcggatggg YJ5023 taccggggagagtaaactgg YJ5024 gtaacactttgtggcgggacc	does not suppress
uev-3(ju587)	3' splice g→a	YJ3849 ttatatttttcgcaataaacag YJ3850 ttgtatttgaatttttaaagtg, cut with TspRI	suppresses
uev-3(ju593)	3' splice g→a	YJ3849 ttatatttttcgcaataaacag YJ3850 ttgtatttgaatttttaaagtg; sequence nt change	suppresses
uev-3(ju638)	3' splice g→a	YJ3847 aaccacaaccacgaaaaacg YJ3848 ggtggaaaagtcaggcaatg; sequence nt change	suppresses
uev-3(ju639)	26 bp deletion in exon 6	YJ7021 attcagtgggacatgcgtgg YJ7022 ccagaacgtagaaatcttgctc	suppresses

uev-3(RNAi) in *eri-1; rpm-1; muIs32* causes suppression of *rpm-1* defects: PLM synapse branch defect 3.2%, PLM hooking 61.3%, ALM hooking 2.2%. n=93 animals, from two independent RNAi test

TABLE S2

DNA expression constructs

Construct name	Insert description
pCZ729 [pENTR-uev-3]	*uev-3* cDNA was generated as RT-PCR product using YJ3852 ggggacaagtttgtacaaaaaagcaggctccaaaatgtccgatcaacctgg and YJ3853 ggggaccactttgtacaagaaagctgggttatgaaattccaatgacatc
pOF163 [Puev-3-GFP]	*uev* operon promoter (1766bp) was amplified using YJ3887 ggggacaagtttgtacaaaaaagcaggctttcgagatgtgacctggc and YJ3935 ggggaccactttgtacaagaaagctgggtccattttctaaatacaaatttg and cloned into *pCZGY32 (pPD9579vGFP_GtwyB).*
pCZ730 [Punc-25-GFP::UEV-3]	An entry clone containing *uev-3* cDNA [*pCZ729 pENTR-uev-3* cDNA] recombined with a destination vector containing 1.2kb of the *unc-25* promoter and GFP labeled at the N-terminus.
pOF111 [Puev-3-uev-3]	6kb Eco 105I - Spe I fragment of cosmid F26H9 was subcloned into pSL1190, containing 1.8kb promoter of the operon, the *rab-5* gene and *uev-3* gene
pOF112 [Prgef-1-uev-3]	An entry clone containing *uev-3* cDNA [*pCZ729 pENTR-uev-3* cDNA] recombined with a destination vector containing 3.5kb of the *rgef-1* promoter.
pOF113 [Prgef-1-PMK-3::GFP]	GFP was amplified and inserted into the *DraIII* site of vector containing 3.5kb of the *rgef-1* promoter and *pmk-3* cDNA, resulting in C-terminal fusion of GFP
pCZ731 [Punc-25-uev-3]	An entry clone containing *uev-3* cDNA [*pCZ729 pENTR-uev-3* cDNA] recombined with a destination vector containing 1.2kb of the *unc-25* promoter.
pOF166 [Pmyo-3-uev-3]	An entry clone containing *uev-3* cDNA [*pCZ729 pENTR-uev-3* cDNA] recombined with a destination vector containing ?kb of the *myo-3* promoter.
pOF176 [pBTM116-UEV-3]	An entry clone containing *uev-3* cDNA [*pCZ729 pENTR-uev-3* cDNA] recombined with a yeast expression destination vector containing the LexA DNA binding domain.
POF177 [pACT2-PMK-3(wt)]	An entry clone containing *pmk-3* cDNA recombined with a yeast expression destination vector containing the Gal4 activation domain.
pOF178 [pACT2-DLK-1]	An entry clone containing *dlk-1* gene [*pOF181 pENTR-dlk-1*] recombined with a yeast expression destination vector containing the Gal4 activation domain.
pOF179 [pACT2-MKK-4]	An entry clone containing *mkk-4* cDNA [*pOF180 pENTR-mkk-4*] recombined with a yeast expression destination vector containing the Gal4 activation domain.
pCZGY971 [Prgef-1-UEV-3(UEV-1 UEV)]	An entry clone containing *uev-3* cDNA was digested with *BamHI* and *SmaI* to remove UEV domain. *uev-1* UEV domain was amplified by PCR and inserted into *uev-3* entry clone. Entry clone was then recombined with destination vector containing *Prgef-1*.
pCZGY973 [Prgef-1-uev-1]	*uev-1 cDNA*, as described in (GUDGEN *et al.* 2004), was cloned into a destination vector containing *Prgef-1*.

TABLE S3

Strains and transgenic constructs

Strains	Transgene and Plasmid [DNA concentration]	Genotype
OF34	*ixEx2 [*pOF163 *Puev-3-GFP* 10ng/µl + pRF4 50ng/µl]	*ixEx2*
OF46	*ixEx3 [*pOF111 *Puev-3-uev-3* 1ng/µl + 50ng/µl pRF4]	*uev-3(ju587); rpm-1(ju44); juIs1; ixEx3*
OF47	*ixEx4 [*pOF112 *Prgef-1-uev-3* 1ng/µl + 50ng/µl pRF4+ 50 ng/µl ttx-3-RFP]	*uev-3(ju587); rpm-1(ju44); juIs1; ixEx4*
OF49	*ixEx6 [*pOF166 *Pmyo-3-uev-3* 1ng/µl + 50ng/µl pRF4+ 50 ng/µl ttx-3-RFP]	*uev-3(ju587); rpm-1(ju44); juIs1; ixEx6*
OF51	*ixEx10 [*pCZ731 *Punc-25-uev-3* 1ng/µl + 50ng/µl pRF4+ 50 ng/µl ttx-3-RFP]	*uev-3(ju587); rpm-1(ju44); juIs1; ixEx10*
C3442	*juEx490 [mkk-4(+)* PCR 5ng/µl + 50 ng/µl ttx-3-GFP]	*juIs1; juEx490*
CZ3694	*juEx490[mkk-4(+)* PCR 5ng/µl + 50 ng/µl ttx-3-GFP]	*dlk-1(ju476); juIs1; juEx490*
CZ4397	*juEx490 [mkk-4(+)* PCR 5ng/µl + 50 ng/µl ttx-3-GFP]	*pmk-3(ju485) juIs1; juEx490*
CZ6072 *juEx490*	*juEx490 [mkk-4(+)* PCR 5ng/µl + 50 ng/µl ttx-3-GFP]	*uev-3(ju587); rpm-1(ju44); juIs1; juEx490*
CZ4168	*juEx669 [mkk-4(STDD)* 5ng/µl + 50 ng/µl ttx-3-RFP]	*juIs1; juEx669*
CZ4215	*juEx669 [mkk-4(STDD)* 5ng/µl + 50 ng/µl ttx-3-RFP]	*dlk-1(ju476); juIs1; juEx669*
CZ4398	*juEx669 [mkk-4(STDD)* 5ng/µl + 50 ng/µl ttx-3-RFP]	*pmk-3(ju485) juIs1; juEx669*
CZ6073	*juEx669 [mkk-4(STDD)* 5ng/µl + 50 ng/µl ttx-3-RFP]	*uev-3(ju587); rpm-1(ju44); juIs1; juEx669*
CZ8808	*juEx1685 [*pCZGY971 *Prgef-1-uev-3(UEV-1 UEV)* 12ng/µl + 50ng/µl ttx-3-RFP]	*uev-3(ju639); muIs32; rpm-1(ju44); juEx1685*
CZ8911	*juEx1685 [*pCZGY971 *Prgef-1-uev-3(UEV-1 UEV)* 12ng/µl + 50ng/µl ttx-3-RFP]	*muIs32; juEx1685*
CZ8831	*juEx1697 [*pCZGY973 *Prgef-1-uev-1* 12ng/µl + 50 ng/µl ttx-3-RFP]	*uev-3(ju639); muIs32; rpm-1(ju44); juEx1697*
CZ12000	*juEx1697 [*pCZGY973 *Prgef-1-uev-1* 12ng/µl + 50 ng/µl ttx-3-RFP]	*muIs32; juEx1697*
CZ9478	*juEx1972 [*pCZGY977 *Pmec-4-uev-3* 10ng/µl + 50 ng/µl ttx-3-RFP*]*	*uev-3(ju639); muIs32; rpm-1(ju44); juEx1972*
CZ11737	*juEx2582 [*pOF166 *Pmyo-3-uev-3* 1ng/µl + 50ng/µl pRF4+ 50 ng/µl ttx-3-RFP]	*uev-3(ju639); muIs32; rpm-1(ju44); juEx2582*
CZ4175	*juEx675 [*pmk-3-DraIII-GFP 50ng/µl + 50ng/µl pRF4]	*juEx675*
OF26	*juEx675 [*pmk-3-DraIII-GFP 50ng/µl + 50ng/µl pRF4]	*uev-3(ju587); juEx675*